Available online at www.sciencedirect.com
ScienceDirect
Pattern Recognition 40 (2007) 659–669
PATTERN RECOGNITION
THE JOURNAL OF THE PATTERN RECOGNITION SOCIETY
www.elsevier.com/locate/patcog

A numerical recipe for accurate image reconstruction from discrete orthogonal moments

Bulent Bayraktar[a, b, c, *], Tytus Bernas[b, c, d, e], J. Paul Robinson[b, c, d, f], Bartek Rajwa[b, c, d]

[a] *School of Electrical and Computer Engineering, Purdue University, West Lafayette, IN 47907, USA*
[b] *Bindley Bioscience Center, Purdue University, 1203 West State St., West Lafayette, IN 47907, USA*
[c] *Cytometry Laboratories, Purdue University, West Lafayette, IN 47907, USA*
[d] *Department of Basic Medical Sciences, Purdue University, West Lafayette, IN 47907, USA*
[e] *Department of Plant Anatomy and Cytology, Faculty of Biology and Protection of Environment, University of Silesia, Jagiellonska 28, Katowice, Poland*
[f] *Weldon School of Biomedical Engineering, Purdue University, West Lafayette, IN 47907, USA*

Received 18 December 2005; received in revised form 10 March 2006; accepted 16 March 2006

Abstract

Recursive procedures used for sequential calculations of polynomial basis coefficients in discrete orthogonal moments produce unreliable results for high moment orders as a result of error accumulation. This paper demonstrates accurate reconstruction of arbitrary-size images using full-order (orders as large as the image size) Tchebichef and Krawtchouk moments by calculating polynomial coefficients directly from their definition formulas in hypergeometric functions and by creating lookup tables of these coefficients off-line. An arbitrary precision calculator is used to achieve greater numerical range and precision than is possible with software using standard 64-bit IEEE floating-point arithmetic. This reconstruction scheme is content and noise independent.

Keywords: Discrete moment; Orthogonal moment; Tchebichef moment; Krawtchouk moment; Reconstruction; Universal image quality index; Arbitrary precision arithmetic

1. Introduction

Moment functions have been used as tools to extract and quantify intrinsic information (e.g., patterns) contained in images (Fig. 1). Moments were introduced in the continuous domain more than four decades ago to digital image processing mainly as a means of performing shape recognition (e.g., for optical character recognition). Today, continuous moments such as geometric, Zernike, pseudo-Zernike, and Legendre are pivotal in many areas of image processing and analysis [1–7]. Practical implementations of continuous orthogonal moments in digital image analysis involve two main sources of error [2,3,8–10]: (i) discrete approximation of the continuous integrals, and (ii) transformation of the image coordinate system into the domain of the polynomials (e.g., transformation from Cartesian to polar coordinates for Zernike moments).

The development of moments led to their discrete versions (e.g., Tchebichef and Krawtchouk moments) and they are overtaking the use of their continuous-domain counterparts because discrete moments offer interesting qualities. First, discretization error [2,3,10,11], which is inherent in implementations of continuous-domain moments, does not play a role in discrete moments, and this fact ensures that discrete moments better satisfy orthogonality and invariance properties. Second, reconstruction of images from discrete orthogonal moments produces better results and is easier to perform using matrix algebra [12,13]. Furthermore, a much-less-mentioned property, the need for thresholding (inherent in continuous-moment applications [5]) after reconstruction is eliminated or minimized. Consequently, higher

* Corresponding author. Bindley Bioscience Center, 1203 West State St., West Lafayette, IN 47907, USA. Tel.: +1 765 409 5627; fax: +1 765 496 1518.
E-mail address: bayrakta@ecn.purdue.edu (B. Bayraktar).

0031-3203/$30.00
doi:10.1016/j.patcog.2006.03.009

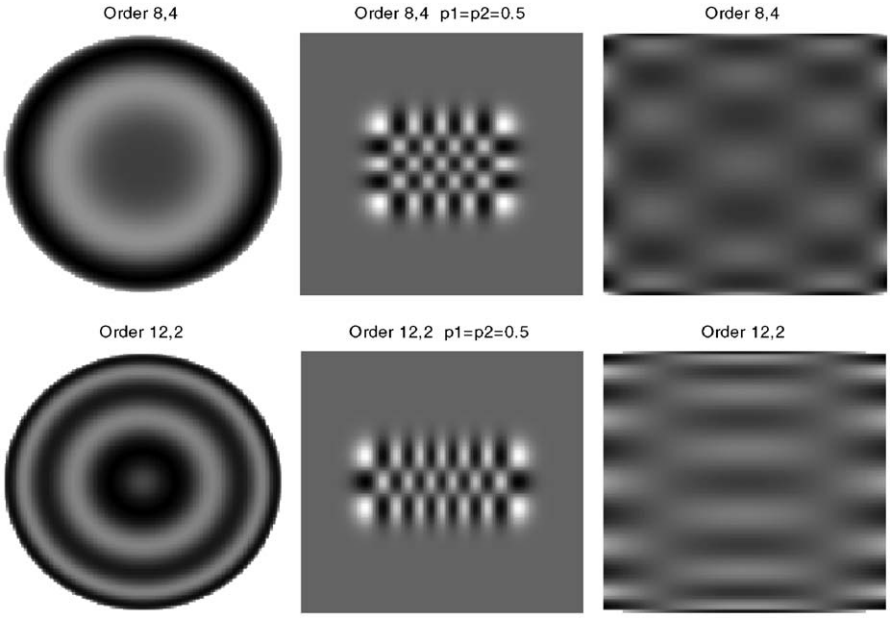

Fig. 1. Two-dimensional representations (size 128 × 128) of three important orthogonal polynomials of various orders: continuous-domain orthogonal Zernike moments [3,11,14] are global features (they give information about the whole image) and are specifically good for capturing circular features (owing to the patterns of Zernike polynomials). Discrete-domain orthogonal Tchebichef (Chebyshev) moments [8,9,15] also give information on global characteristics in images, and discrete-domain orthogonal Krawtchouk moments [13] can be applied locally to extract local information.

reconstruction fidelity could potentially be obtained when discrete moments are used. This is important because reconstruction fidelity is used as a metric for the accuracy of the moment values from which the original image is retrieved [2,14]. Therefore, if the reconstruction fidelity is high, the moment values can be judged to be more precise. However, an important problem with discrete moments is that polynomial coefficients of discrete moments are usually calculated using recurrence equations, which leads to propagation and accumulation of numerical errors with increasing moment order and image size. This effect precludes perfect image reconstruction since description of all the info in an image is possible only through computation of all moments up to the size of the image. Attempts to solve the numerical instability problems include indirect solutions such as use of a block-wise scheme to perform reconstruction in subsections of an image [12], which obviates the need to use higher-order moments. In the case of Tchebichef moments, other methods performed modification of the recursive procedure to construct orthonormal versions of Tchebichef polynomials by modifying the scale factor involved [15], or used Clenshaw's recurrence formula to improve the accuracy and speed [16]. However, noisy conditions cause instability in these methods as well.

It is shown here that computation of discrete moments employing arbitrary precision solves the problem of numerical instability. However, it is also obvious that such an approach would be a computational challenge, rendering such a method infeasible for image analysis and processing applications. The only practical way to implement such computations in real time is to use some form of lookup table (LUT). Herein we propose a simple, yet robust and practical method of achieving faultless reconstruction of images, performed using the full spectrum (maximum size of image allowed as the highest order of moments) of discrete orthogonal moments such as Tchebichef and Krawtchouk. This is attained by calculating discrete polynomial coefficients directly from their definitions rather than using their recurrence relationships and by constructing LUTs of polynomial basis coefficients. These coefficients can be stored and retrieved later for use. The reconstruction fidelity is verified by two image-quality metrics: root-mean square error (RMSE) and universal image quality index (UIQI) [17].

The organization of the paper is as follows: Section 2 covers the mathematical background. It reviews the formulation of discrete orthogonal Krawtchouk and Tchebichef moments from their respective discrete polynomials and includes the definition of universal image quality index as an image reconstruction fidelity metric. It also covers details on numerical precision arithmetic. Section 3 identifies and demonstrates the numerical instability problems in image reconstruction from discrete orthogonal moments. Section 4 provides solution to the problems set forward in Section 3 with examples. Section 5 contains conclusions for this work.

2. Mathematical background

2.1. Discrete orthogonal moments

For a 2D continuous function $f(x, y)$, moments have the general form $M_{pq} = \int\int f(x, y)h_{pq}(x, y)\,\mathrm{d}x\,\mathrm{d}y$ where $h_{pq}(x, y)$ is a polynomial in x and y with powers p and q,

respectively. The different polynomials lead to various types of moments. If $f(x, y)$ is a digital image, then an approximation of this integral is used: $M_{pq}=\sum_x\sum_y f(x, y)h_{pq}(x, y)$. This discretization step is the source of errors in calculation of continuous-domain moments.

2.1.1. Krawtchouk polynomials and moments

Krawtchouk moments [13] are a set of moments formed by using discrete Krawtchouk polynomials as the basis function set. The nth order classical Krawtchouk polynomial is defined as

$$K_n(x; p, N) = \sum_{k=0}^{N} a_{k,n,p}x^k = {}_2F_1\left(-n, -x; -N; \frac{1}{p}\right), \quad (1)$$

where $x, n = 0, 1, 2, \ldots, N$, $N > 0$, $p \in (0, 1)$. ${}_2F_1$ is the hypergeometric function defined as

$${}_2F_1(a, b; c; z) = \sum_{k=0}^{\infty} \frac{(a)_k(b)_k}{(c)_k}\frac{z^k}{k!} \quad (2)$$

and $(a)_k$ is the Pochhammer symbol given by $(a)_k = a(a + 1)\ldots(a + k - 1) = \Gamma(a + k)/\Gamma(a)$. The set of $(N + 1)$ Krawtchouk polynomials $\{K_n(x; p, N)\}$ forms a complete set of discrete basis functions with weight function $w(x; p, N) = \binom{N}{x}p^x(1 - p)^{N-x}$ and satisfies the orthogonality condition

$$\sum_{x=0}^{N} w(x; p, N)K_n(x; p, N)K_m(x; p, N)=\rho(n; p, N)\delta_{nm}, \quad (3)$$

where $n, m = 1, 2, \ldots, N$ and $\rho(n; p, N) = (-1)^n((1 - p)_n/p)n!/(-N)_n$. The following recurrence relation:

$$-xK_n(x; p, N) = p(N - n)K_{n+1}(x; p, N) - [p(N - n) + n(1 - p)]K_n(x; p, N) + n(1 - p) \times K_{n-1}(x; p, N) \quad (4)$$

is used to calculate higher-order Krawtchouk polynomials. A normalization process is applied to eliminate large variability in the dynamic range. The set of normalized (weighted) Krawtchouk polynomials $\{\overline{K}_n(x; p, N)\}$ is defined by [13]

$$\overline{K}_n(x; p, N) = K_n(x; p, N)\sqrt{\frac{w(x; p, N)}{\rho(n; p, N)}}. \quad (5)$$

The Krawtchouk moment of order $(n + m)$ in terms of weighted Krawtchouk polynomials, for an $N \times N$ image with intensity function $f(x, y)$, is defined as

$$Q_{nm}=\sum_{x=0}^{N-1}\sum_{y=0}^{M-1}\overline{K}_n(x; p_1, N-1)\overline{K}_m(y; p_2, M-1)f(x, y). \quad (6)$$

The image intensity function, $f(x, y)$, can be written (the image can be reconstructed) completely in terms of the Krawtchouk moments (up to a certain order) as

$$f(x, y)=\sum_{x=0}^{N-1}\sum_{y=0}^{M-1}Q_{nm}\overline{K}_n(x; p_1, N-1)\overline{K}_m(y; p_2, M-1). \quad (7)$$

Another property of Krawtchouk moments is their ability to characterize the local properties (in a region of interest) of images. The parameters p_1 and p_2 are used to shift the region of interest horizontally and vertically [13]. In matrix form [13], thanks to the separability of the 2D Krawtchouk polynomials into 1D, the Krawtchouk moment matrix, Q, is defined as $Q = K_2AK_1^{\mathrm{T}}$ where T denotes the transpose

$$Q = \{Q_{ji}\}_{i,j=0}^{i,j=N-1},$$
$$K_v = \{\overline{K}_i(j; p_v, N - 1)\}_{i,j=0}^{i,j=N-1},$$
$$A = \{f(j, i)\}_{i,j=0}^{i,j=N-1}. \quad (8)$$

The image is reconstructed by $A = K_2^{\mathrm{T}}QK_1$ (using up to a certain order of Krawtchouk moments). Calculations are performed more easily (e.g., using Matlab) by such matrix manipulations.

2.1.2. Tchebichef polynomials and moments

The discrete Tchebichef polynomials are defined as [9]

$$t_n(x) = (1 - N)_n\ {}_3F_2(-n, -x, 1 + n; 1, 1 - N; 1), \quad n, x, y = 0, 1, 2, \ldots, N - 1, \quad (9)$$

where $(a)_k$ is the Pochhammer symbol given by

$$(a)_k = a(a + 1)\ldots(a + k - 1) = \frac{\Gamma(a + k)}{\Gamma(a)} \quad (10)$$

and ${}_3F_2$ is the hypergeometric function defined as

$${}_3F_2(a_1, a_2, a_3; b_1, b_2; z) = \sum_{k=0}^{\infty}\frac{(a_1)_k(a_2)_k(a_3)_k(b)_k}{(b_1)_k(b_2)_k}\frac{z^k}{k!}. \quad (11)$$

The Tchebichef polynomials satisfy the orthogonality property

$$\sum_{x=0}^{N-1} t_m(x)t_n(x) = \rho(n, N)\delta_{mn}, \quad 0\leqslant m,\ n\leqslant N - 1 \quad (12)$$

with

$$\rho(n, N) = \frac{N(N^2 - 1)(N^2 - 2^2)\ldots(N^2 - n^2)}{2n + 1} = (2n)!\binom{N + n}{2n + 1}, \quad n = 0, 1, \ldots, N - 1$$

and have the following recurrence relation:

$$(n + 1)t_{n+1}(x) - (2n + 1)(2x - N + 1)t_n(x) + n(N^2 - n^2)t_{n-1}(x) = 0, \quad n = 1, 2, \ldots, N - 1. \quad (13)$$

Scaled Tchebichef moments are introduced [9] with the scaling constant $\beta(n,N)=N^n$ as $\tilde{t}_n(x)=t_n(x)/\beta(n,N)$, which leads to the modification $\tilde{\rho}(n,N)=\rho(n,N)/(\beta(n,N))^2$. Tchebichef moments then can be defined as [8,9]

$$T_{pq}=\frac{1}{\rho(p,N)\rho(q,N)}\sum_{x=0}^{N-1}\sum_{y=0}^{N-1}\tilde{t}_p(x)\tilde{t}_q(x)f(x,y),$$
$$p,q=0,1,2,\ldots,N-1. \tag{14}$$

This equation also leads to the following inverse moment transform, which can be used for faithful (with accuracy proportional to the higher order of moments used) reconstruction of the original image:

$$f(x,y)=\sum_{m=0}^{N-1}\sum_{n=0}^{N-1}T_{mn}\tilde{t}_m(x)\tilde{t}_n(x),$$
$$x,y=0,1,\ldots,N-1. \tag{15}$$

Reconstruction from Tchebichef moments can be made more easily in matrix form in exactly the same way as the Krawtchouk moments. The scaling factor can be modified to calculate orthonormal versions of Tchebichef moments [15].

2.2. Numeric precision in computations

2.2.1. ANSI/IEEE standard 754-1985 for binary floating-point arithmetic

Nonzero floating-point numbers are normalized, which means they can be expressed as [18] $x=\pm(1+f)\cdot 2^e$. The quantity f is the fraction or *mantissa* and e is the *exponent*. The fraction satisfies $0\leqslant f<1$ and the exponent e is an integer in the interval $-1022\leqslant e\leqslant 1023$. Any numbers that do not meet these limitations must be approximated by ones that do [18,19]. The finiteness of f is a limitation on *precision* and this leads to *roundoff* errors. The finiteness of e is a limitation on *range* and this leads to *overflow* and *underflow*. Double-precision floating-point numbers are stored (on 32-bit systems) in 64-bit words, with 52 bits for f, 11 bits for e, and one bit for the sign of a number. The sign of e is accommodated by storing $e+1023$, which is between 1 and $2^{11}-2$ (1 and 2046). The entire fractional part is not f, but $1+f$, which has 53 bits. However, the leading 1 does not need to be stored. The computer integer resolution (the maximum unsigned floating-point integer) is $\eta=2^{53}-1=9.007199254740991\times 10^{15}$. Therefore, any pair of numbers that have the same exponent but whose mantissas differ by less than η^{-1} have the same representation. This is how *roundoff* errors arise [6].

IEEE double-precision uses *eps* as the distance from 1 to the next larger floating-point number, where $eps=2^{-52}\approx 2.220446049250313\times 10^{-16}$. The smallest positive normalized floating-point number has $f=0$ and $e=-1022$. The largest floating-point number has f a little less than 1 and $e=1023$. MATLAB calls these numbers *realmin* and *realmax*. Together with *eps*, they characterize the standard system [6,18,19].

$$\text{realmin}=2^{-1022}=2.225073858507201\times 10^{-308},$$
$$\text{realmax}=(1+(1-eps))\times 2^{1023}$$
$$=1.797693134862316\times 10^{308}.$$

If any computation tries to produce a value larger than *realmax*, it is said to *overflow* and the result is an exceptional floating-point value called *infinity* or *Inf*. If any computation tries to produce a value that is undefined even in the real number system, the result is an exceptional value known as Not-a-Number or *NaN*. If any computation tries to produce a value smaller than *realmin*, it is said to *underflow*. This involves one of the optional and controversial aspects of the IEEE standard [18]. Many, but not all, machines allow exceptional denormal or subnormal floating-point numbers in the interval between *realmin* and $eps*realmin$ (this is the case for MATLAB). Therefore, the smallest positive subnormal number is about $4.940656458412465\times 10^{-324}$. Any results smaller than this are set to 0.

2.2.2. Arbitrary-precision arithmetic

In arbitrary-precision arithmetic, integers and floating-point numbers are, respectively, represented as

$$I_a=\sum_{i=0}N_p^iB^i \quad\text{and}\quad F_a=\sum_{i=0}\frac{N_p^i}{B^i}, \tag{16}$$

where N_p is a fixed precision integer or floating point number and B is the base (e.g., 2, 8, 10, 16). This representation makes it possible to obviate limitations of numerical precision and range imposed by fixed-precision arithmetic, provided that a sufficient number of terms in the above summations is used.

2.3. Universal image quality index (UIQI)

UIQI is universal in the sense that it does not take the viewing conditions or the individual observer into account. UIQI is designed to model any image distortion as a combination of three factors: loss of correlation, luminance distortion, and contrast distortion [17]. The index takes values between -1 and 1 with 1 being the best. In two dimensions, let x be the original image and y be the test (corrupted) image. Then,

$$\text{UIQI}=\frac{\sigma_{xy}}{\sigma_x\sigma_y}\cdot\frac{2\bar{x}\bar{y}}{(\bar{x})^2+(\bar{y})^2}\cdot\frac{2\sigma_x\sigma_y}{\sigma_x^2+\sigma_y^2}$$
$$=\frac{4\sigma_{xy}\bar{x}\bar{y}}{[(\sigma_x^2+\sigma_y^2)((\bar{x})^2+(\bar{y})^2)]}, \tag{17}$$

where $\bar{x}$, $\bar{y}$ are the average intensity values of the images and σ_x^2, σ_y^2, σ_{xy} are the local variances and covariances of x and y images.

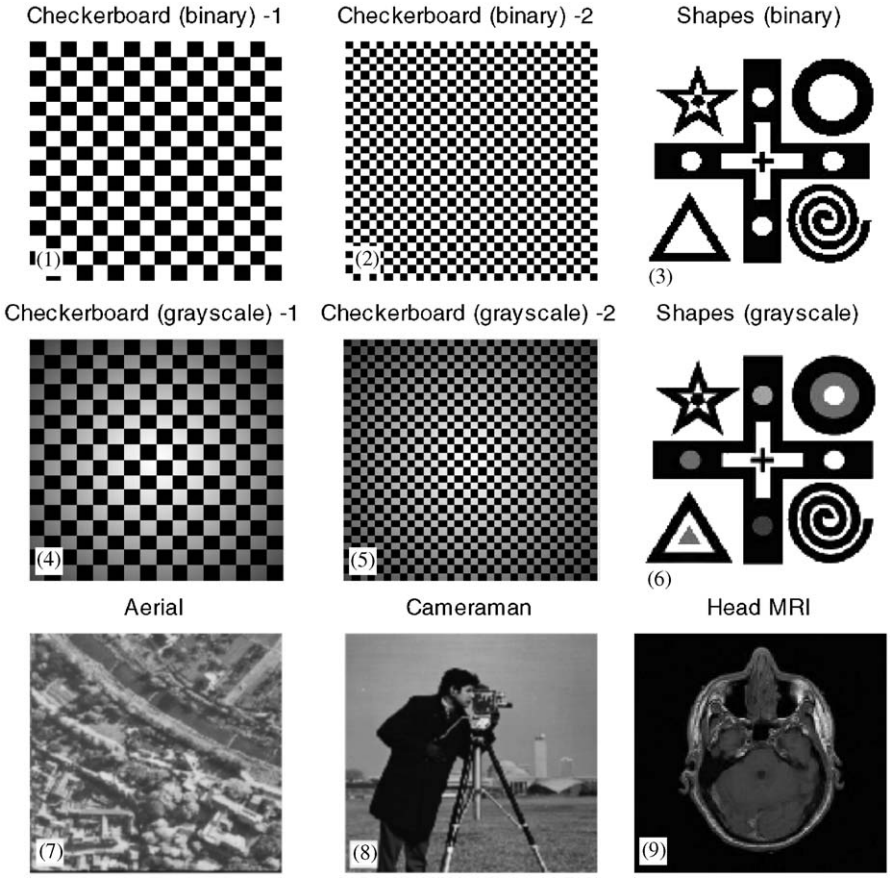

Fig. 2. Various synthetic, natural, and medical test images (binary and gray-scale).

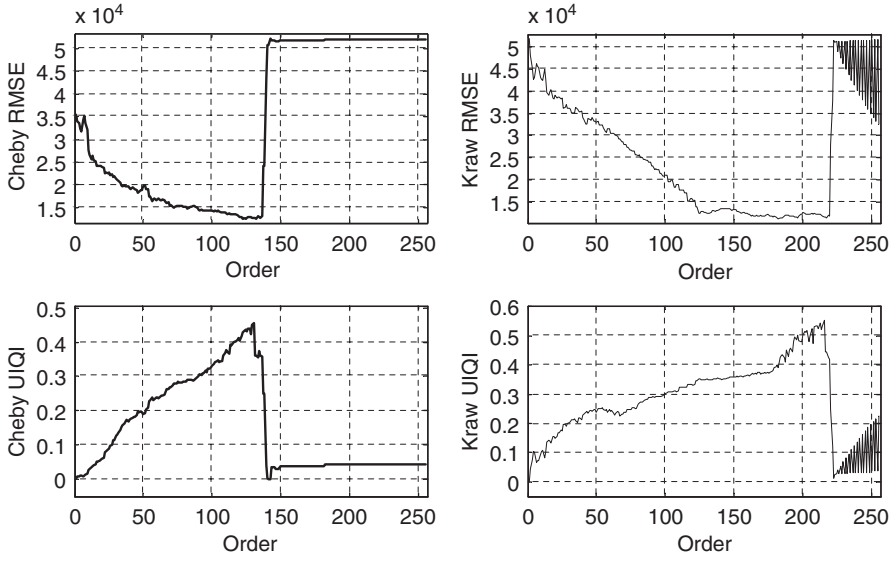

Fig. 3. Image quality for reconstruction of 'Shapes' (binary) via Tchebichef and Krawtchouk moments with recurrence relations.

3. Numerical instabilities in discrete moments

It is clear from the equations of different types of polynomials that lead to various moments that as the moment order or the image size increases the numbers involved grow dramatically. For example, $t_n(x)$ and $K_n(x)$ are polynomials in x^n, and the dynamic range of values will have huge variations with either large x ($0 < x < N-1$, image size $N \times N$) or

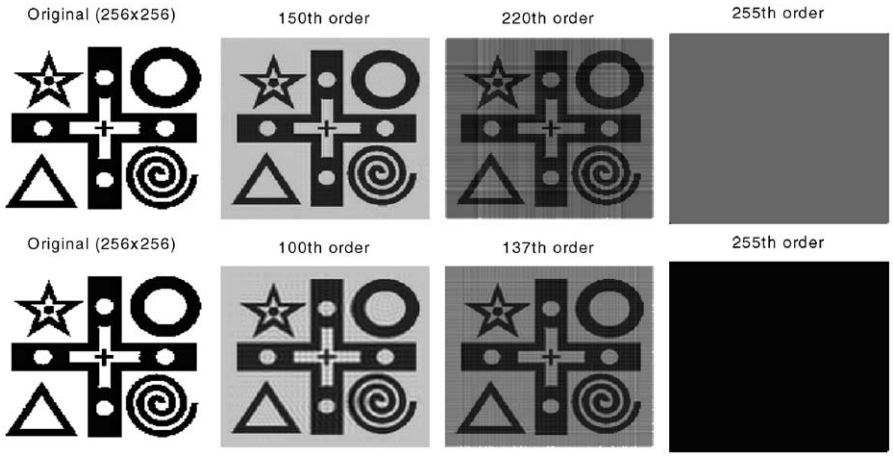

Fig. 4. 'Shapes' image (binary) used for reconstruction via Krawtchouk (first row) and Tchebichef (second row) moments without LUTs.

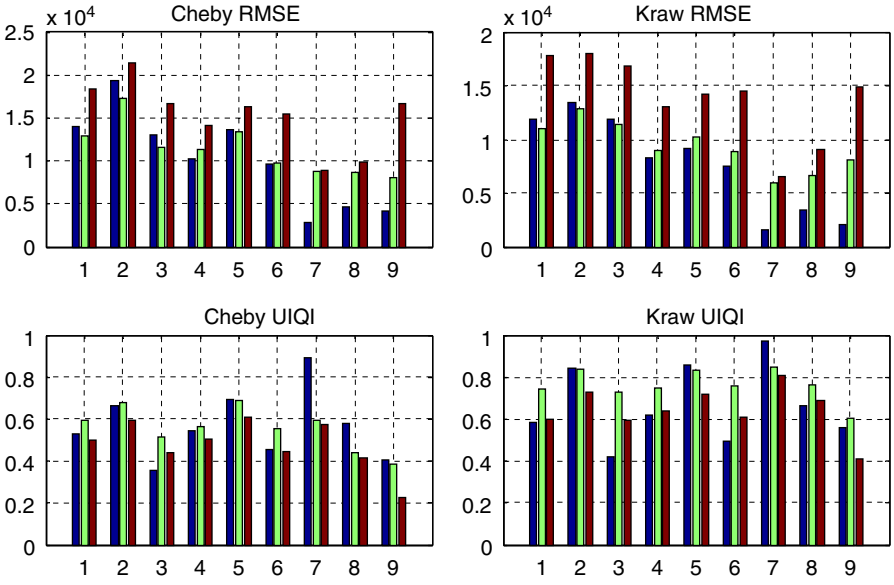

Fig. 5. Maximum image quality for reconstruction of test images (Fig. 2) using recurrence relations of Tchebichef and Krawtchouk polynomials. For each image, there is also a version with added Gaussian and Salt&Pepper noise, in this order (left to right), used for reconstruction.

large n (order of moment). Real numerical problems (in calculation of Krawtchouk and Tchebichef moments) lie with multiplication of Pochhammer symbols and use of factorials. Large values from the results of these operations cannot be stored using 64-bit signed integers (double precision on 32-bit systems), which offer a range of (approximately) $\pm 10^{19}$. Larger numbers can be stored with loss of precision using 64-bit IEEE floating-point standard as explained in detail in Section 2.2.1. However, this storage capacity may prove insufficient even in the case of relatively small images (e.g., 128×128 pixels) making the calculations ill conditioned. In addition, division of these large values (necessary to compute hypergeometric functions), even if technically possible, may not be handled accurately using 64-bit arithmetic. Therefore, numeric instabilities are bound to occur. The problems of storage and division of these large values can be obviated using recursive calculation of polynomial coefficients. However, the recursive scheme results in error accumulation. Consequently, precise computation of even a 100th-order moment may not be achieved in practice using this scheme. Therefore, the full spectrum of moments (where maximum moment order = maximum size of image) cannot be used in practice and the fidelity of image reconstruction is doomed to be low.

The numerical instability in image reconstruction using discrete moments is demonstrated in Figs. 2–5, and 11. Calculation of RMSE and UIQI (Fig. 3) demonstrates that for 256×256 images, reconstruction with discrete orthonormal Tchebichef polynomials [15] loses stability at order 136 and with Krawtchouk polynomials at order 219. In 128×128

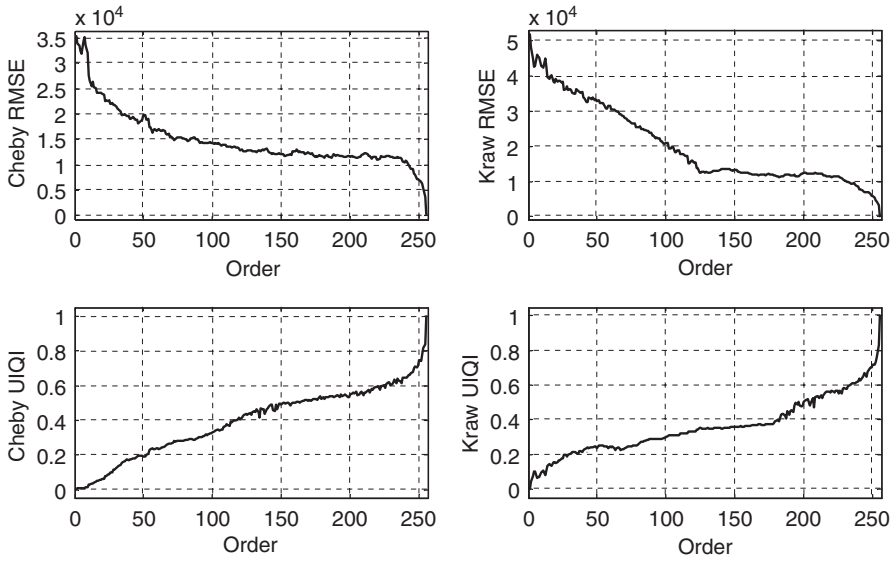

Fig. 6. Image quality for reconstruction of 'Shapes' (binary) via Tchebichef and Krawtchouk moments with LUTs.

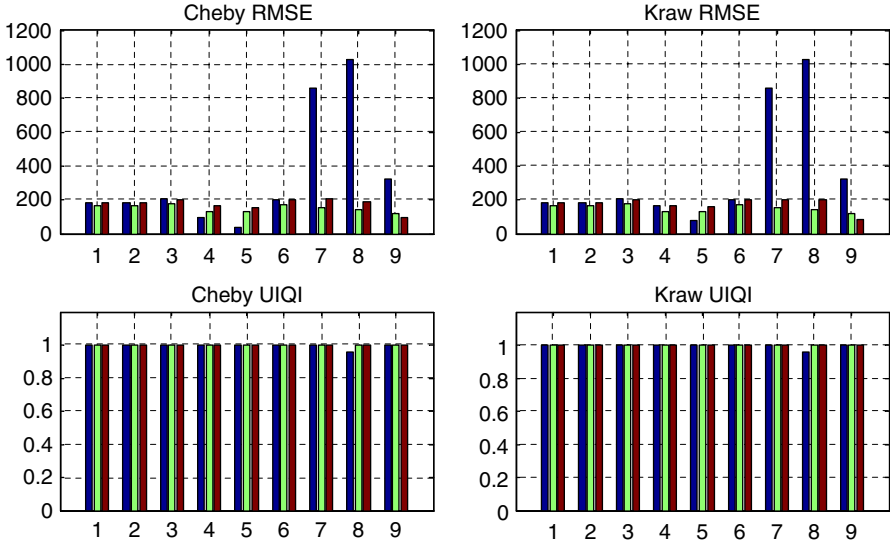

Fig. 7. Maximum image quality achieved for reconstruction of all test images (Fig. 2) using LUTs. For each image, there is also a version with added Gaussian and Salt&Pepper noise (same noise as in images in Fig. 5), in this order (left to right), used for reconstruction.

images, these orders are 97 and 124, respectively (data not shown). Fig. 4 shows (for binary 'Shapes' image) the reconstructed images at the point right after the recurrence relations start to fail visually; lines begin to appear in reconstructed images after order 219 for Krawtchouk moments and 136 for Tchebichef moments. Hence, beyond these limits, image quality of the reconstruction does not improve but instead degrades significantly. Fig. 5 displays (for all test images used in Fig. 2) the RMSE and UIQI for reconstructed images using both Krawtchouk and Tchebichef moments with orders at their breaking points (219 and 136, respectively). It can be seen that, although the same order is used for reconstruction, the image quality varies substantially among different images in both metrics. This shows that not only does the reconstruction using recurrence relations have a limited success but also this success is content-dependent.

4. Problem solution and experimental results

In order to eliminate the need for recursive moment calculation we used GNU bc (basic calculator) software [20] (with base 10) that has arbitrary numeric precision capability. We avoided renormalization of the recursive relations and calculated the Krawtchouk and Tchebichef polynomial coefficients directly from their definitions [9,13,21] in hypergeometric functions (in Eqs. (2) and (11)). We calculated

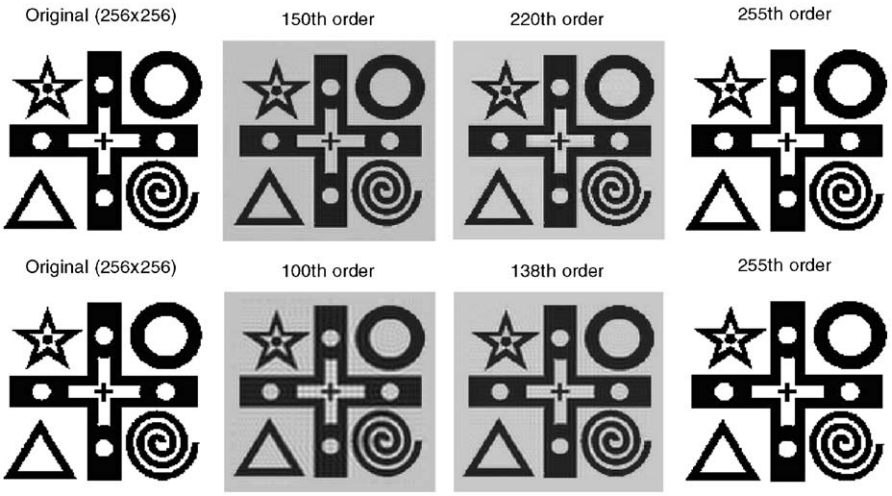

Fig. 8. 'Shapes' image (binary) used for reconstruction via Krawtchouk (first row) and Tchebichef (second row) moments with LUTs.

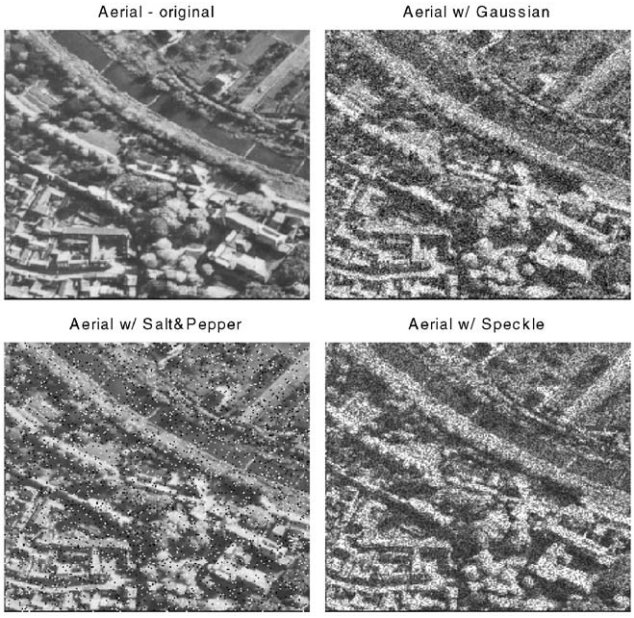

Fig. 9. Aerial image with various noise (Gaussian with SNR = 12, Salt&Pepper SNR = 12, and Speckle SNR = 13).

the coefficients for a set of image sizes up to 512 × 512 and formed LUTs. The LUTs were applied for decomposition and subsequent reconstruction. This technique made it possible to obtain faithful reconstruction of an image from its respective sets of moments, as demonstrated in Figs. 6–10, and 12. This process has two advantages: it produces very accurate reconstruction results, and even though the computations using the arbitrary precision calculator are much slower than the recurrence scheme (since LUTs are formed off-line in advance, stored and retrieved later), the decomposition and reconstruction are performed rapidly in practice.

We used several images (binary and gray-scale) with different types and content to demonstrate our approach. We present here the results for the images in Fig. 2. Fig. 6 shows the image quality of exact reconstruction with discrete Krawtchouk and Tchebichef moments using LUTs; the image quality continues to increase and reaches the minimum/maximum possible (0 for RMSE and 1 for UIQI) by both quality criteria. Fig. 7 shows the image quality, which is much better than that obtained without LUTs, attained for all test images at order 255 (maximum order possible) using LUTs. Fig. 8 shows an example of such a reconstruction. Fig. 10 shows the same trend as in previous figures for an aerial image with various noise types (Gaussian, Salt&Pepper, Speckle) that are added artificially (in Fig. 9). The direct calculation of the polynomial coefficients, which leads to LUTs, is faithfully able to retrieve the details (high-frequency components) of the original images and noise as the image quality metrics continue to increase/decrease, whereas reconstruction without LUTs fail at a certain order (as mentioned above, 219 for Krawtchouk and 136 for Tchebichef moments; bold and thick lines represent reconstruction quality without using LUTs and thin lines show reconstruction with LUTs).

Fig. 11 shows a trend for the 512 × 512 cameraman image similar to that shown for 256 × 256 images. Image reconstruction (for the 512 × 512 cameraman image) from Krawtchouk moments using recurrence relations begins to show significant visual degradation when (up to) 390th-order moments are used. Tchebichef moments suffer similar fatal degradation starting around (up to) 195th order. Fig. 12 shows that all the above problems can be solved using the solution proposed in this paper.

Tables 1 and 2 show a numerical comparison between sample elements of (Tchebichef) 128 × 128 T1 matrices, calculated using fixed-precision and arbitrary-precision arithmetic (where 65 digits after decimal point is used), respectively. T1 matrices were constructed similar to the Krawtchouk polynomial coefficient matrices (Eq. (8)). Using fixed-precision numbers, the calculations fail to produce

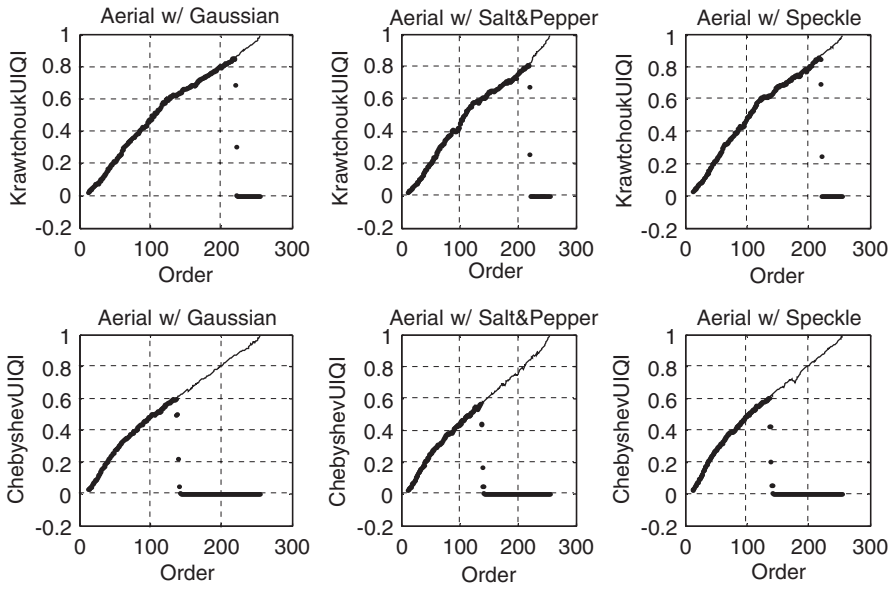

Fig. 10. UIQI on reconstruction of aerial image with various noise (Fig. 9) using recurrence relations (dark lines) and LUTs (thin lines).

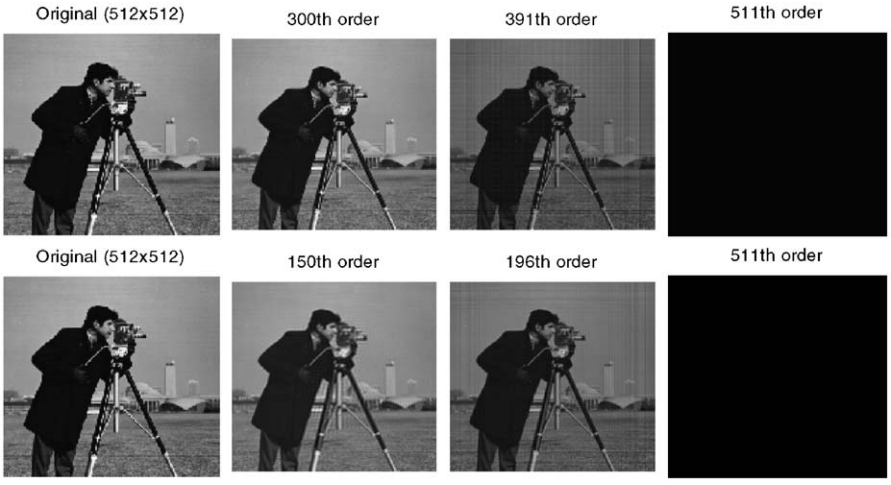

Fig. 11. 'Cameraman' image (512 × 512) used for reconstruction via Krawtchouk (first row) and Tchebichef (second row) moments without LUTs.

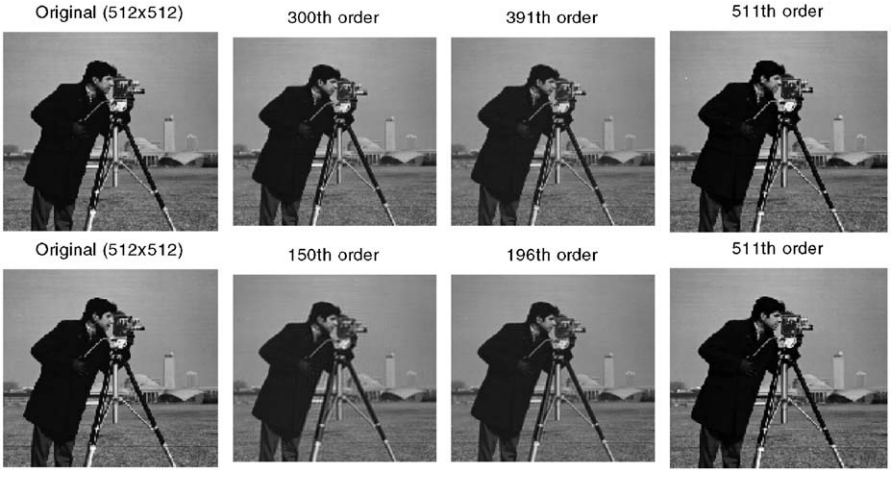

Fig. 12. 'Cameraman' image (512 × 512) used for reconstruction via Krawtchouk (first row) and Tchebichef (second row) moments with LUTs.

Table 1
Sample elements of the 2D Tchebichef polynomial matrix (128 × 128) with fixed-precision arithmetic

T1	112	118	122
112	$3.883133971546536 \times 10^{-8}$	$6.899999754031292 \times 10^{-6}$	0.07152881861427
118	$7.444829697101211 \times 10^{-8}$	0.00700245916439	$1.212700579919720 \times 10^{2}$
122	$2.694365402757248 \times 10^{-6}$	0.43695029358600	$1.043217733319892 \times 10^{4}$

Table 2
Sample elements of the 2D Tchebichef polynomial matrix (128 × 128) with arbitrary-precision arithmetic (in fixed-precision format of Matlab)

T1	112	118	122
112	$3.865328927993463 \times 10^{-8}$	$8.202945491700744 \times 10^{-13}$	$7.114574118322008 \times 10^{-17}$
118	$5.029784792226311 \times 10^{-11}$	$4.555247927459617 \times 10^{-16}$	$2.400877599188298 \times 10^{-20}$
122	$2.097849876633264 \times 10^{-13}$	$1.122713158805788 \times 10^{-18}$	$4.327564934163435 \times 10^{-23}$

meaningful results (instead of very small numbers, large numbers are obtained for higher-order moment element in the matrix). It should be mentioned that although our results are very accurate, they are not perfect as can be seen from some error residues shown by the image quality metrics in Fig. 7. This can be easily attributed to the fact that even though the arbitrary-precision arithmetic (65 digits after the decimal point) is used for the calculations and the results are stored in LUTs, the reconstruction process uses these LUTs in Matlab, which can retain only up to 16 digits after the decimal point.

5. Conclusions

The use of discrete orthogonal Krawtchouk and Tchebichef moments eliminates inherent errors that exist in continuous-domain moments, offers better representation of image content, and hence allows better image reconstruction. However, the moments suffer from accumulating error owing to the use of polynomial recursion in their calculations. This paper gives an accurate reconstruction scheme via formation of LUTs from direct calculation of polynomial coefficients of discrete moments using an arbitrary precision calculator. Additionally, through examples covering various images (binary, gray-scale, medical, checker-pattern, etc.), this simple yet efficient method is shown to be universal, robust, content independent, and noise independent.

References

[1] M. Hu, Visual pattern recognition by moment invariants, IRE Trans. Inf. Theory 8 (1962) 179–187.
[2] S.X. Liao, M. Pawlak, On image analysis by moments, IEEE Trans. Pattern Anal. Mach. Intell. 18 (1996) 254–266.
[3] S.X. Liao, M. Pawlak, On the accuracy of Zernike moments for image analysis, IEEE Trans. Pattern Anal. Mach. Intell. 20 (1998) 1358–1364.
[4] A. Khotanzad, Y.H. Hong, Invariant image recognition using features selected via a systematic method, Pattern Recognition 23 (1990) 1089–1101.
[5] S.P. Prismall, M.S. Nixon, J.N. Carter, On moving object reconstruction by moments, Proceedings of British Machine Vision Conference, 2002, pp. 1–10.
[6] J. Martinez, F. Thomas, Efficient computation of local geometric moments, IEEE Trans. Image Process. 11 (2002) 1102–1111.
[7] J. Flusser, J. Boldys, B. Zitova, Moment forms invariant to rotation and blur in arbitrary number of dimensions, IEEE Trans. Pattern Anal. Mach. Intell. 25 (2003) 234–246.
[8] R. Mukundan, S.H. Ong, P.A. Lee, Discrete versus continuous orthogonal moments in image analysis, International Conference on Imaging Science Systems and Technology, vol. 1, 2001, pp. 23–29.
[9] R. Mukundan, S.H. Ong, P.A. Lee, Image analysis by Tchebichef moments, IEEE Trans. Image Process. 10 (2001) 1357–1364.
[10] C.H. Teh, R.T. Chin, On digital approximation of moment invariants, Comput. Vision Graph. Image Process. 33 (1986) 318–326.
[11] A. Khotanzad, Y.H. Hong, Invariant image recognition by Zernike moments, IEEE Trans. Pattern Anal. Mach. Intell. 12 (1990) 489–497.
[12] N.A. Abu, N. Suryana, R. Mukundan, Perfect image reconstruction using discrete orthogonal moments, Proceedings of Fourth IASTED International Conference on Visualization, 2004, pp. 903–907.
[13] P.T. Yap, R. Paramesran, S.H. Ong, Image analysis by Krawtchouk moments, IEEE Trans. Image Process. 12 (2003) 1367–1377.
[14] C.H. Teh, R.T. Chin, On image analysis by the methods of moments, IEEE Trans. Pattern Anal. Mach. Intell. 10 (1988) 496–513.
[15] R. Mukundan, Some computational aspects of discrete orthonormal moments, IEEE Trans. Image Process. 13 (2004) 1055–1059.
[16] G. Wang, S. Wang, Recursive computation of Tchebichef moment and its inverse transform, Pattern Recognition 39 (2006) 47–56.
[17] Z. Wang, A.C. Bovik, A universal image quality index, IEEE Signal Proc. Lett. 9 (2002) 81–84.
[18] C.B. Moler, Numerical Computing with Matlab, Society for Industrial and Applied Mathematics, 2004, pp. 34–42.
[19] IEEE standard for binary floating-point arithmetic, ANSI/IEEE Std 754-1985, IEEE Standards Board and American National Standards Institute, 1985.
[20] BC—Interactive Algebraic Language, ⟨http://directory.fsf.org/GNU/bc.html⟩.
[21] R. Koekoek, R.F. Swarttouw, The Askey-Scheme of hypergeometric orthogonal polynomials and its q-Analogue, Technische Universiteit Delft Faculty of Technical Mathematics and Informatics Report 98-17, 1998, Delft, Netherlands.

About the Author—BULENT BAYRAKTAR received B.S. and M.S. degrees in electrical engineering and applied physics from Case Western Reserve University, Cleveland, OH, USA, in 1999. He received his Ph.D. in electrical and computer engineering from Purdue University in 2006. His interests are feature extraction, image analysis, and pattern recognition in biological and medical applications.

About the Author—TYTUS BERNAS received an M.S. (with honors) in biology in 1996 and a Ph.D. in biophysics in 2003, both from Jagiellonian University, Krakow, Poland. He has been an assistant professor at the University of Silesia, Katowice, Poland since 2003. From 2004 to 2006 he was a post-doctoral research scientist at Purdue University, West Lafayette, USA.

About the Author—J. PAUL ROBINSON has a B.Sc., M.Sc., and Ph.D. all from the University of NSW in Sydney, Australia. In 1993 he was appointed Professor of Immunopharmacology at Purdue University, and in 1999 Professor of Biomedical Engineering. He currently serves in both the Department of Basic Medical Sciences in the School of Veterinary Medicine and the Weldon School of Biomedical Engineering at Purdue University, West Lafayette, IN, USA. He is the director of Cytometry Laboratories in Bindley Bioscience Center within the newly formed interdisciplinary Discovery Park on the Purdue main campus.

About the Author—BARTEK RAJWA received an M.S. (with honors) in molecular biology in 1996 and a Ph.D. in biophysics in 2003, both from Jagiellonian University, Krakow, Poland. He is a Senior Research Scientist in the Cytomics and Imaging Research Core of the Bindley Bioscience Center at Purdue University. His research focuses on applications of various optical methods to biological imaging of cells and tissues.